PAPER

Room temperature synthesis of PbSe quantum dots in aqueous solution: stabilization by interactions with ligands

Oliva M. Primera-Pedrozo,*[a] Zikri Arslan,*[a] Bakhtiyor Rasulev[b] and Jerzy Leszczynski[b]

An aqueous route of synthesis is described for rapid synthesis of lead selenide quantum dots (PbSe QDs) at room temperature in an attempt to produce water-soluble and stable nanocrystals. Several thiol-ligands, including thioglycolic acid (TGA), thioglycerol (TGC), 3-mercaptopropionic acid (MPA), 2-mercaptoethylamine hydrochloride (MEA), 6-mercaptohexanoic acid (MHA), and L-cysteine (L-cys), were used for capping/stabilization of PbSe QDs. The effects of the ligands on the stability of PbSe QDs were evaluated for a period of two months at room temperature under normal light conditions and at 4 °C in the dark. The TGA- and MEA-capped QDs exhibited the highest stability prior to purification, almost two months when kept in the dark at 4 °C. However, the stability of TGA-capped QDs was reduced substantially after purification to about 5 days under the same conditions, while MEA-capped QDs did not show any significant instability. The stabilization energies of Pb–thiolate complexes determined by theoretical DFT simulations supported the experimental results. The PbSe QDs capped with TGA, MPA and MEA were successfully purified and re-dispersed in water, while those stabilized with TGC, MHA and L-cys aggregated during purification attempts. The purified PbSe QDs possess very susceptible surface resulting in poor stability for about 30–45 min after re-dispersion in water. In the presence of an excess of free ligand, the stability increased up to 5 days for TGA-capped QDs at pH 7.19, 9–12 days for MPA-capped QDs at pH 7.3–7.5 and 45–47 days for MEA-capped QDs at pH 7.35. X-Ray diffraction (XRD) results showed that the QDs possess a cubic rock salt structure with the most intense peaks located at $2\theta = 25.3°$ (200) and $2\theta = 29.2°$ (100). TEM images showed that the size of the QDs ranges between 5 and 10 nm. ICP-MS results revealed that Pb : Se ratios were 1.26, 1.28, 3.85, 1.18, and 1.31 for the QDs capped with TGA, MPA, MEA, L-cys, and TGC, respectively. The proposed method is inexpensive, simple and utilizes environmentally friendly chemicals and solvents.

1. Introduction

In recent years, lead selenide quantum dots (PbSe QDs) have attracted much interest due to their infrared optical properties caused by the transitions occurring in the NIR wavelength range ($\lambda = 1.1$–4.0 μm).[1–4] These semiconductor nanocrystals belong to the IV–VI group and have extensive applications in solar cells,[5] telecommunication devices,[6] photodetectors,[7] and biomedical labeling.[8] The conventional syntheses of PbSe QDs use hazardous organo-metallic precursors and high boiling-point organic solvents, such as tri-*n*-octylphosphine/tri-*n*-octylphosphine oxide (TOP/TOPO).[1,3,9] These approaches yield QDs capped with organic (hydrophobic) ligands that are not suitable for biological applications. Other non-aqueous syntheses

reported for PbSe QDs involve the use of a microwave-assisted polyol process,[10] a hydrothermal process,[11] and a solvothermal synthesis using octadecylamine.[12] In these methods the final products are not only insoluble in water, but also the fabrication involves the use of toxic solvents that are not desirable for environmental and biological applications.[13]

To promote water solubility, the organic ligands can be exchanged with water-soluble groups, such as mercaptocarbonic-acids[14] (TGA or MPA) or polymer[15,16] (PEG-NH$_2$) coatings to have hydrophilic capping on the surfaces of the nanocrystals. However, one disadvantage of ligand exchange is that physical or optical properties of the QDs are altered that inevitably[17] decreases their efficiency for the desired applications. For instance, oleic acid-stabilized PbSe QDs have been transferred from organic phase into water by exchanging hydrophobic oleate cap with hydrophilic 11-MUA (mercaptoundecanoic acid).[2] Although there was no apparent change in the absorption after ligand exchange, the results showed that the quantum yield emission decreased from 89% to 35%. Similar behavior was

[a] *Jackson State University, Department of Chemistry and Biochemistry, Jackson, MS, 39217, USA. E-mail: zikri.arslan@jsums.edu; olivaprimera@yahoo.es; Fax: +1 (601)979 3674; Tel: +1 (601)9791618*
[b] *Interdisciplinary Center for Nanotoxicity, Department of Chemistry and Biochemistry, Jackson State University, Jackson, MS, 39217, USA*

observed by Etgar *et al.*[18] in the stabilization of PbSe QDs by 2-aminoethanethiol (AET), where the QDs were prepared in organic phase, and then TOP surface-binding was replaced by AET to produce water soluble QDs.

Another largely unknown point concerning the ligand exchange attempts is the stability of the PbSe QDs in water, especially after the purification and re-dispersion in water.[19] Despite the feasibility of exchanging the organically soluble ligands with water-soluble counterparts, the extent of the stability of the resulting PbSe QDs has not been examined in detail yet.

An alternative to overcome the difficulties associated with ligand exchange processes is the synthesis of PbSe QDs in aqueous medium. In this study, experimental studies have been conducted to achieve direct synthesis of PbSe QDs in water in an attempt to develop an environmentally friendly route of synthesis. Several thiol ligands were utilized and their performances were investigated for effective stabilization of QDs in aqueous solution. Emphasis was given to the effects of purification and the effects of free ligands on the stability of purified PbSe QDs.

2. Materials and methods

2.1 Reagents and solutions

Deionized water (17.8 MΩ cm) obtained by dual purification through reverse osmosis membrane coupled to a Barnstead E-pure system was used. Lead acetate, $Pb(Ac)_2 \cdot 3H_2O$ (99.0–103%), and selenium powder (99+%) were purchased from Alfa Aesar. Thioglycolic acid (TGA, ≥98%), 3-mercaptopropanoic acid (MPA, 99+%), 6-mercaptohexanoic acid (MHA, 90%), thioglycerol (TGC, 98%), 2-mercaptoethylamine hydrochloride (MEA, 98+%), L-cysteine (L-cys, ≥97%), sodium borohydride ($NaBH_4$, ≥98%) and dimethyl sulfoxide (DMSO, ACS reagent) were purchased from Sigma Aldrich. 5.0 M sodium hydroxide solution was made from NaOH pellets (99.9%, Sigma Aldrich). Trace metal grade hydrochloric acid (HCl, Fisher Scientific) and nitric acid (HNO_3, Fisher Scientific) were used for preparation of selenium stock solution and digestion of the samples. Acetone and 2-propanol (ACS reagent) were obtained from Fisher Scientific.

Selenium powder (4 g) was dissolved in concentrated HNO_3 (1.0 g samples in separate polypropylene tubes) to prepare Se(IV) solution. After dissolution, the solvent in the tube was evaporated to remove excess nitric acid. The contents in each tube were then combined and diluted to 100 mL with 10% v/v HCl to reduce Se(VI) to Se(IV) in solution. The final concentration of the Se(IV) stock was 0.5 M. Sodium borohydride solution (10%, m/v) was prepared freshly by dissolving 1.0 g $NaBH_4$ in 0.1% m/v NaOH solution.

2.2 Synthesis of PbSe QDs

All glassware used in synthesis was cleaned with freshly prepared aqua regia (HCl : HNO_3, 3 : 1 by volume) and rinsed thoroughly in water prior to use. The QDs were synthesized by using aqueous solutions of Se(IV) and lead acetate trihydrate ($Pb(Ac)_2 \cdot 3H_2O$) as selenium and lead sources, respectively. Some parts of the procedure and set-up were adopted from the protocols used for the synthesis of CdTe QDs[20] and CdSe QDs[21] in aqueous solutions. The thiol stabilizers and the optimal working pHs are summarized in Table 1. In a typical synthesis, approximately 0.190 g of lead acetate trihydrate were dissolved in 250 mL of ultra pure water in a three-neck flask (flask-1) followed by the addition of 0.5 mL of TGA as capping ligand under vigorous stirring. The solution was first turbid due to the poor solubility of the lead–thiolate complex which dissolved by raising the pH with 5.0 M sodium hydroxide (NaOH) solution. Into a separate three-neck flask (flask-2), 2.5 mL of the 0.5 M Se(IV) solution and 2.5 mL of 10% v/v HCl were added, which was then connected to flask-1 (see Fig. 1) *via* a Teflon tubing (*e.g.* transfer tubing). Both flasks were tightly connected with septa and purged with nitrogen (N_2) for 30 min under stirring. Hydrogen selenide gas (H_2Se) was generated by drop-wise addition of 10 mL of a freshly prepared 10% w/v $NaBH_4$ (in 0.1% m/v NaOH) into flask-2 using a 10 mL plastic syringe as described elsewhere.[21] Under constant N_2 flow, the H_2Se was continuously transferred to flask-1 and reacted with Pb–thiolate complex. The formation of PbSe QDs occurred instantaneously at room temperature indicated by a change in the color of the solution from colorless to black. Nitrogen was purged for an additional 20 min. Stirring was performed at room temperature for another 1 h after stopping N_2 flow to ensure the formation of stable nanocrystals.

To determine the colloidal stability, each QDs solution was split into two equal portions. One portion was kept at room temperature (under normal light exposure) while the second portion was wrapped by aluminium foil and stored in the dark at 4 °C in a refrigerator. The stability of each suspension was examined visually for coagulation (*e.g.*, aggregation) for over a period of two months at both conditions. The information collected formed the dataset for experimental stability (see Section 3.3 and Table 4). Photochemical stability and the stability of optical properties were not investigated in this study.
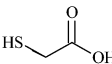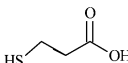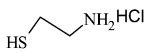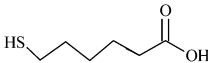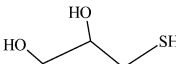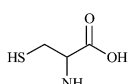
2.3 Purification

Different solvents, including DMSO, acetone and 2-propanol, were used for purification of the PbSe QD solutions. Dimethyl sulfoxide (DMSO) was used for QDs capped with TGA and MPA. In a typical protocol, 25 mL of PbSe QDs solution was added to a 50 mL polypropylene centrifuge tube and immersed in an ice bath for 15 min. Then, 25 mL of DMSO was added while shaking gently. The tubes were kept in the ice bath for another 10 min and then centrifuged. Details of the other ligands are discussed in the Results and discussion section. For all the ligands, samples were centrifuged at 6000 rpm for 30 min. Finally, the supernatant was carefully removed and the pellet was washed with acetone and then immediately re-dispersed in water and in an excess of free ligand at different pHs to affect the stability of purified QDs suspension. Coagulation or formation of precipitate at the bottom of the tube was monitored as a measure of colloidal stability.

2.4 ICP-MS analysis of PbSe QDs and precursor solutions

The molar concentrations of lead and selenium in the QD solutions were determined by ICP-MS using a Varian 820MS

Table 1 Thiol stabilizing agents and pH conditions used for aqueous synthesis of PbSe QDs at room temperature

Ligand	Chemical structure	pH
Thioglycolic acid (TGA)		10.0–10.1
3-Mercaptopropanoic acid (MPA)		10.0–10.1
2-Mercaptoethylamine hydrochloride (MEA)		5.1–10.1
6-Mercaptohexanoic acid (MHA)		11.1–11.3
Thioglycerol (TGC)		10.1–11.2
L-Cysteine (L-cys)		10.0–10.1
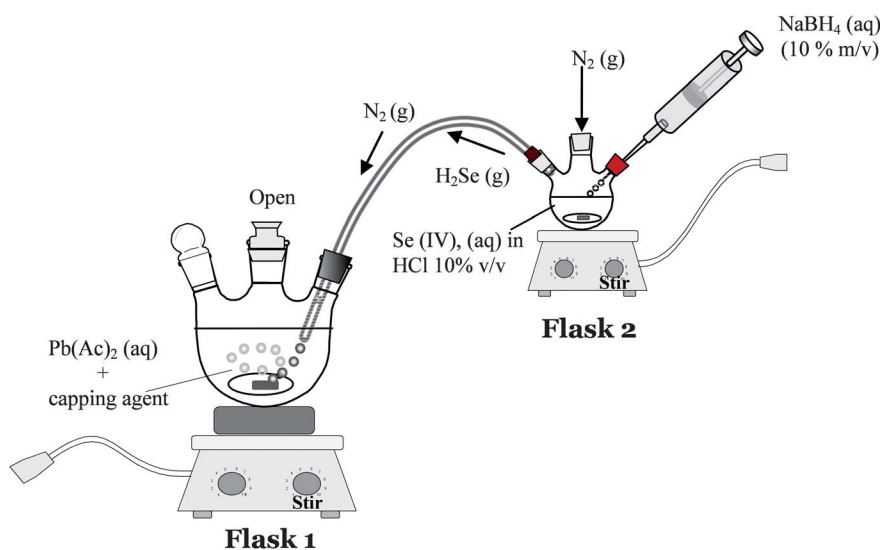
Fig. 1 Schematic representation of the experimental setup for aqueous synthesis of thiol-capped PbSe QDs at room temperature.

ICP-MS instrument (Varian, Australia). For determination, 1.0 mL of the QD solutions ($n = 4$) were purified as described above with DMSO. The supernatant was carefully removed and the QDs residue was dissolved with 1.0 mL of concentrated HNO_3 by heating at 100 °C for 5–10 min. The solutions were completed to 4 mL with water.

For determination of impurities in the precursor solutions, 50 µL of 0.5 M Se(IV) stock solution ($n = 3$) was placed in a 15 mL polypropylene tube followed by addition of 5 mL of 10% v/v HNO_3 and completed to 10 mL with water. For the lead acetate solution, 50 mg samples ($n = 3$) were placed in 15 mL tubes and dissolved with 5 mL of 5% v/v HNO_3 solution, and then diluted to 10 mL with water. All solutions (purified PbSe QDs and selenium and lead acetate) were further diluted 100-fold with deionized water and analyzed by ICP-MS to determine the concentrations of Pb, Se and impurities. Quantification was performed by using ^{206}Pb and ^{208}Pb isotopes for Pb, and ^{78}Se and

^{82}Se isotopes for Se. The concentrations for Pb and Se are reported as the average ± standard deviation of the two isotopes.

2.5 Characterization of PbSe QDs

X-Ray diffraction (XRD) and FTIR measurements were made with powders of the QDs. To obtain the powders, purified QD samples were rinsed with acetone and dried at room temperature. XRD patterns were recorded by a Rigaku Ultima III X-Ray diffractometer equipped with a Cu-Kα target ($\lambda = 0.15418$ nm). X-Ray profiles were recorded in the 2θ range of 20–90° at room temperature by operating the anode using a 40 kV voltage and 44 mA current. The scanning speed and step were 1° min^{-1} and 0.02°, respectively.

The shape and size of the QDs were characterized by transmission electron microscopy (TEM) by using a JEOL JEM-2100 TEM instrument. TEM samples were prepared by spotting

a drop of a 1 : 10 diluted QDs solution on a CF300-Cu grid (Electron Microscopy Sciences). The TEM images were recorded at an accelerating voltage of 200 kV.

Fourier Transform Infrared Spectroscopy (FTIR) was used to verify the binding of the ligands on the QDs surface. A Bruker Optics micro-FTIR IFS/vs spectrometer equipped with a DTGS infrared detector was used to record the FTIR spectra of the samples of pure ligands. Spectra were collected using OPUS Version 4.2 (Bruker software) in the range of 4000–500 cm^{-1}, at 10 scans and 4 cm^{-1} resolution. For recording FTIR spectra of the QD powders, a Shimadzu IRAffinity-1 FTIR instrument in ATR mode was used at 4 cm^{-1} resolution and 45 scans within the same spectroscopic range (4000–500 cm^{-1}).

2.6 Computational details

All calculations were performed with the Gaussian 03 program code.[22] Due to the large amount of the calculations to be performed, we have selected the most efficient quantum mechanical method. Density functional theory-based electronic structure calculation is a computationally economical approach ensuring high power for predicting structural and thermodynamic properties of various species.[23] Taking into account the relatively large systems and types of metal atoms to be calculated, including transition metal atoms, the density functional theory (DFT) method was chosen to calculate the stabilization energies of Pb and the ligands. The Minnesota functional M05 method developed by Truhlar group[24] was selected among the various density functional modules. The 6-31G(d,p) basis set, except for the effective core potential (ECP) basis set LANL2DZ (Los Alamos National Lab effective core potential with double zeta basis set for valence electrons), for transition metal (e.g., Pb)[25] was applied in this study. The computational approach consisted of: (1) optimization of the ligands in anionic form; (2) calculation of the interaction of Pb atom with the ligands to estimate the stability of the system; and (3) calculation of stabilization energy and comparison of the data.

3. Results and discussion

3.1 Characterization of PbSe QDs

Thiol-stabilized PbSe nanocrystals were produced in aqueous solution at room temperature by the reaction of Pb–thiolate complexes with $H_2Se(g)$ using the thiol agents as shown in Table 1. The XRD patterns of the PbSe QDs are illustrated in Fig. 2a–d. The molar ratio of ligand to Pb^{2+}, [ligand]/[Pb^{2+}], was 22 throughout the syntheses unless otherwise indicated differently. The intensity and positions of the peaks are in very good agreement with the reported values.[2,3,10] XRD spectra evidence the crystalline structure of the nanocrystals that exhibit eight peaks that are assigned to (111), (200), (220), (311), (222), (400), (420) and (422) diffractions corresponding to a rock-salt (NaCl) cubic structure. Typical TEM micrographs of the PbSe QDs are illustrated in Fig. 3. The images indicate small nanocrystals of approximately 5 to 10 nm in size.

The lattice parameter values were 6.105, 6.108, 6.102, 6.092, and 6.111 for TGA-, MEA-, L-cys-, TGC-, and MPA-capped PbSe QDs, respectively. These values are also consistent with the reported values.[26–28] According to the XRD patterns, the degree
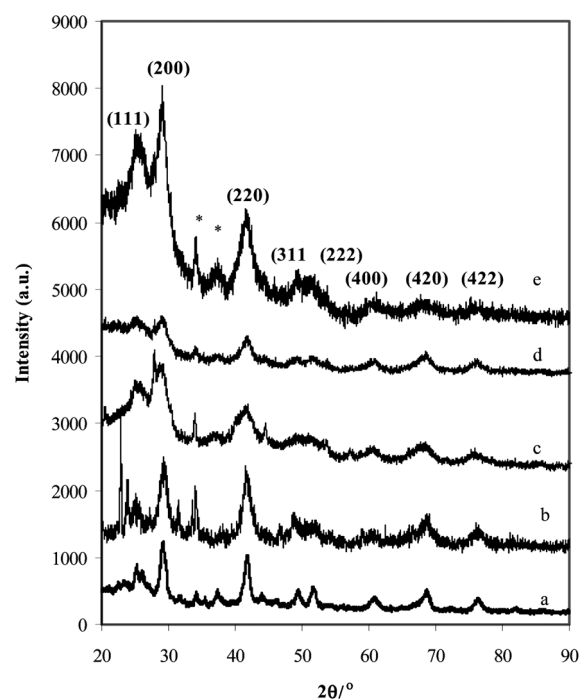

Fig. 2 X-Ray diffraction patterns of PbSe QDs with different cappings. The [ligand]/[Pb^{2+}] molar ratio is 22. (a) TGA; (b) MEA; (c) L-cys; (d) TGC; (e) MPA.
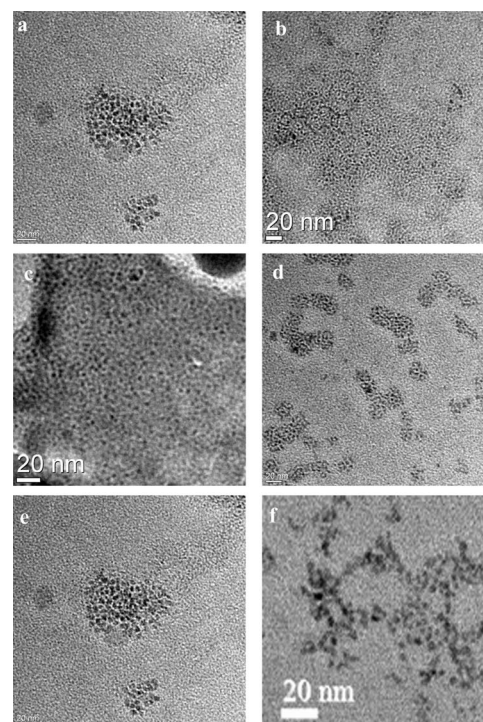

Fig. 3 TEM images of PbSe QDs with different ligands. (a) MPA; (b) TGA; (c) L-cys; (d) TGC; (e) MHA; (f) MEA. The [ligand]/[Pb^{2+}] ratio is 22.

of crystallinity was better when TGA was used as the ligand. The sharpening of the XRD peaks confirmed the formation of highly crystalline PbSe QDs. Additional peaks (asterisks) observed at

2θ values of 31° and 38° were thought to associate with excess Pb atoms at the surface of the QDs as confirmed by ICP-MS characterization of the QDs (see Section 3.2). In the case of L-cys-capped QDs (Fig. 2c), the amount of purified powder was very small, therefore, the extra splitting observed at (200) is likely a spike due to reflection from the sample holder.

To elucidate the effect of the length of the carbon chain on the stability, TGA, MPA and MHA were used as test ligands. As we discuss later in this paper, the stabilities of MPA- and MHA-capped PbSe QDs were not comparable to those capped with TGA and MEA. In addition, the synthesis of MHA-capped QDs was costly, and thus it was not possible to produce sufficient amounts of powder through small-scale synthesis to acquire well-defined peaks in X-ray measurements. Attempts with 11-mercaptoundecanoic acid (11-MUA), another long-chain thiol carboxylic acid, were also made. However, the synthesis with 11-MUA was unsuccessful due to the poor solubility of this compound in water even at high pH values.

The FTIR absorption spectra recorded for the thiol ligands on the surface of PbSe QDs are shown in Fig. 4. The band assignments are summarized in Table 2. It is important to note that the S–H vibration located within 2400–2542 cm^{-1} in the spectra of pure (e.g., free) thiol ligands (data not shown) disappeared completely in the FTIR spectra of all capped PbSe QDs regardless of the ligand used (Fig. 4). This result indicates the cleavage of the S–H bond of the ligands and the formation of a new S–Pb bond between the ligand and PbSe nanocrystals. TGA, MPA, MHA and L-cys ligands possess in their chemical structure a C=O functional group. The C=O vibration band is located at ~1700 cm^{-1} (ref. 3,29 and 30) in the pure ligands. However, this vibration shifted to 1657 cm^{-1}, 1663 cm^{-1}, 1662 cm^{-1}, and 1616 cm^{-1} for MPA, TGA, MHA and L-cys,

Table 2 FTIR band assignments for purified PbSe nanocrystals

Assignment	Region/cm^{-1}
ν(C–S)	660–770
C–O stretching	1206–1236
C–N^a	1327, 1074
NH$_2$ scissoring	1582
N–H bend	1500–1640
ν_s(COO$^-$), ν_{as}(COO$^-$)	1400–1663
νCH$_2$	2935–2943

^{a} For PbSe QDs capped with L-cys and MEA, respectively.

respectively. The bands within 1400–1470 cm^{-1} and 1616–1663 cm^{-1} in the spectra of PbSe QDs can be attributed to symmetric ν_s(COO$^-$) and asymmetric ν_{as}(COO$^-$), respectively.

The presence of these bands in the FTIR spectra confirms the existence of carboxylate moieties on the QD surface as found in other studies from the absorption of carboxylic acids on metal surfaces.[31–33] This is an expected result because of the use of basic pH that resulted in deprotonation of the acid to form carboxylate groups while ensuring complete dispersion of the QDs in water through the electrostatic repulsions. Another band located at ~667 cm^{-1} is attributed to the C–S vibration, which clearly demonstrates the presence of ligand (cap) on the surface of the purified PbSe QDs. The –NH$_2$ scissoring mode of MEA was observed at 1582 cm^{-1} as a very sharp peak.[34] In addition, the –CH$_2$ bending and C–N stretching modes are observed in the spectrum and are also provided in Table 2 with corresponding wavenumbers.

3.2 ICP-MS characterization of PbSe QDs

The stoichiometric ratios of Pb and Se obtained from ICP-MS analysis of the PbSe QDs solutions are presented in Table 3. These QDs were synthesized at a [ligand]/[Pb] ratio of 22. The molar ratios for [Pb]/[Se] ranged between 1.18 and 1.31 that were close to the expected theoretical ratio of 1 : 1. In all the cases, however, the PbSe QD samples possessed an excess of Pb. This phenomenon was also manifested in the XRD pattern with the peaks at 2θ values of 31° and 38° (marked with asterisks). The analysis of the precursor solutions showed that both Pb(Ac)$_2$ and Se(IV) solutions were of high purity with no significant levels of metallic impurities, indicating the peaks in XRD spectra could not be from the presence of foreign nanocrystals. Thus, these peaks were thought to correspond to Pb as demonstrated elsewhere by Peng et al.[35]

The non-stoichiometric ratio of Pb and Se in PbSe QDs has been reported before for the nanocrystals (3–8 nm) synthesized
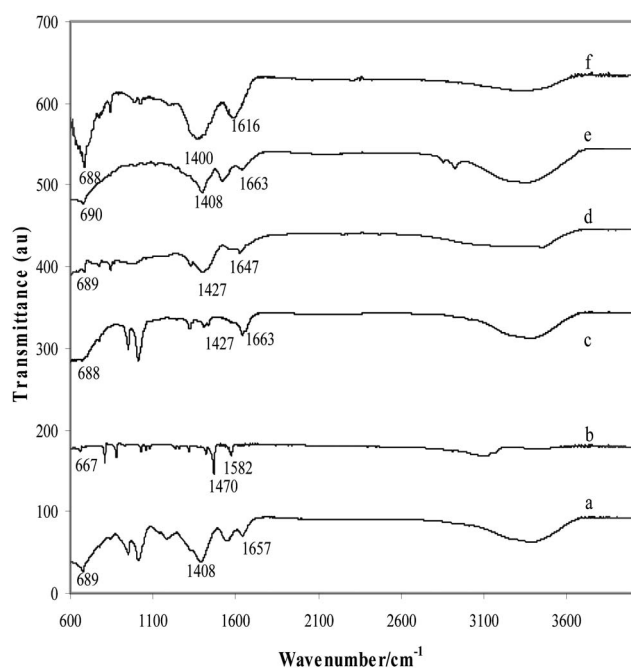

Fig. 4 FTIR spectra of purified PbSe QDs with different ligands. The [ligand]/[Pb^{2+}] ratio is 22. (a) MPA; (b) MEA; (c) TGA; (d) TGC; (e) MHA; (f) L-cys.

Table 3 Elemental composition of Pb and Se in purified PbSe QDs

QD–ligand	Pb/moles	Se/moles	Pb/Se ratio
PbSe–MPA	1.55 ± 0.06	1.21 ± 0.10	1.28
PbSe–TGA	1.06 ± 0.03	0.84 ± 0.06	1.26
PbSe–MEA	4.10 ± 0.20	1.10 ± 0.10	3.85
PbSe–L-cys	1.59 ± 0.06	1.35 ± 0.11	1.18
PbSe–MHA	1.92 ± 0.07	0.50 ± 0.04	3.66
PbSe–TGC	1.85 ± 0.12	1.41 ± 0.12	1.31

by the Murray protocol.[27] This excess of Pb was also confirmed with the ICP-MS measurements (Table 3). The findings from surface chemistry studies of PbSe QDs demonstrated that the excess Pb was indeed present as Pb atoms adsorbed on the QD surface. These Pb atoms were found to oxidize over the time and complex with the excess ligands in the solution.[27,36]

It is important to state at this point that the synthesis of PbSe QDs at acidic or neutral pHs was possible with MEA only. The syntheses performed at basic pH values (∼10.0) resulted in poor stability such that the QDs in most trials aggregated at the reaction stage. This result was due to the fact that the amine (non-ionic) form is present in the alkaline solutions. At neutral (∼7) and acidic pH values, however, the protonated $-NH_3^+$ forms allowing the formation of stable PbSe QDs.

X-Ray diffraction patterns (data not shown) for the samples synthesized at basic pHs did not show the reflections of a rock-salt crystal structure indicating that PbSe QDs did not form. However, for powders from synthesis at neutral pHs, the peaks were observed as expected with an impurity located at $2\theta = 22°$ value. The ICP-MS data showed an excess of Pb (Pb/Se ratio = 3.85) in the QDs as shown in Table 3. This excess of Pb was also observed for MHA-capped PbSe QDs as shown in Table 3.

3.3 Effects of ligands on stability of QDs before purification

The reaction of $H_2Se(g)$ with Pb–thiolate complex was very fast leading to the formation of PbSe nanocrystals in seconds. The QDs are formed when 10% w/v $NaBH_4$ solution is added to flask-2 containing Se(IV) in 10% v/v HCl. Because the $NaBH_4$ reacts very vigorously with Se(IV) in acidic medium, it was critical to add $NaBH_4$ solution slowly to control the nucleation of the nanocrystals and avoid aggregation. Rapid formation of PbSe nanocrystals has been also reported for non-aqueous synthesis using oleic acid (OA) as ligand.[9] It was found that the reaction was completed in 4 min when the ratio between OA/Pb was set at 3/1. We also observed in this study that higher concentration of ligands caused fast growth of PbSe nanocrystals resulting in premature precipitation due to the formation of large nanocrystals in the solution. Thus, the effect of Se(IV) concentration for different ligand/Pb^{2+} ratios was examined on the stability of the PbSe nanocrystals. In these experiments, Pb^{2+} concentration was kept at 0.002 M while ligand concentrations varied from 0.02 to 0.05 M, and that of Se(IV) varied from 0.005 (2.5 mL) to 0.01 M (5.0 mL). The effects of these parameters on the stability were evaluated similarly at room temperature (18–22 °C) and at 4 °C in the dark. The results revealed that the PbSe QDs were more stable when the Pb/Se molar ratio was 0.4 [2.5 mL Se(IV)] than it was 0.2 [5.0 mL Se(IV)]. For instance, for MPA stabilized QDs (ligand/Pb^{2+} = 11), the QDs were stable at room temperature for 10 days at a Pb/Se ratio of 0.4 and 3 days for a Pb/Se ratio of 0.2. The same behavior was observed for MEA-, TGA-, L-cys-, MHA- and TGC-capped nanocrystals, and was related to the rate of formation and size of the nanocrystals. A higher Pb/Se ratio provided relatively slow growth (e.g., reaction) yielding smaller nanocrystals that were more stable. The ligand concentration also affected the stability of the QDs. At a particular Pb/Se ratio (e.g., 0.4), the stability increased when the ligand/Pb^{2+} ratio was increased from 11 to 22.

Photochemical instability has been reported for thiol-capped QD suspensions of CdSe,[14,37] PbS[38] and PbSe synthesized with non-aqueous methods.[39] In this study, the stability of PbSe QDs was evaluated at room temperature (with light) and at 4 °C in darkness (no light). As indicated in Table 4, the relative stability was dependent on the nature of the ligand. TGA–PbSe QDs were stable for about 16–19 days before purification at room temperature. However, the stability increased to about 47–53 days when a portion of the same suspension was kept in the dark at 4 °C. Likewise, MEA–PbSe QDs were found to be stable for almost two months in the dark (4 °C). Although not systematically investigated during the course of the studies, some of the QD suspensions were left unwrapped in the refrigerator at 4 °C. These suspensions were found to be notably less stable than the wrapped suspensions at the same temperature. These observations are consistent with previous reports[14,38,39] and are attributed to the light-induced oxidation/decomposition of the PbSe QDs over the time. However, it should be stated that other factors including, the type of ligand, concentration of the ligand, Pb/Se ratio, and pH were also influential on the stability of the PbSe QDs besides the effects of light and temperature.

The QDs stabilized with MHA-capped (six carbons) are expected to be more stable than those stabilized with TGA or MPA because of the increasing van der Waals interactions between neighboring carbon chains.[14] However, the results showed that MHA-capped QDs were not as stable as the MPA- and TGA-capped QDs. This effect was attributed to the instability of Pb–MHA complex because of the poor solubility of MHA in water compared with the rest of the ligands. The data in Table 4 indicate that MEA provided the best stabilization for PbSe QDs even at room temperature under light exposure. At neutral pHs (7.0–7.35), the QDs were stable for 17–32 days and showed the diffractions corresponding to a rock-salt PbSe cubic structure, but this crystalline structure was not observed at basic pH values. The results presented here suggest a remarkable stability of MEA- (neutral pH) and TGA-capped PbSe QDs compared to the rest of the ligands considered. This phenomenon can be explained by evaluation and comparison of the stabilization energies between Pb^{2+} ion and the ligands (Table 5).

3.4 DFT theoretical studies

Theoretical investigations were performed to find the nature of ligand's effect on stability of the capped QDs. The quantum-

Table 4 The extent of stability recorded for thiol-capped PbSe QDs at room temperature (20–22 °C) and light conditions, and in the dark at 4 °C

| QD–ligand	Stability at room conditions (day)	Stability in the dark (day)
PbSe–TGA	16–19	47–53
PbSe–MEA[a]	17–32	>60
PbSe–MEA[b]	6–9	12–16
PbSe–MHA	9	15–17
PbSe–MPA	8–10	16–21
PbSe–L-cys	6–7	12–15
PbSe–TGC	4–5	15

[a] Synthesis performed at neutral pH values. [b] Synthesis performed at basic pH values.

Table 5 The stability energy E_{ST} and metal–ligand bond lengths R_{M-L} for different ligands

QD–ligand	R_{M-L}/Å	E_{ML}/a.u.	E_{ST}, Δ/a.u.	E_{ST}, Δ/eV
PbSe–MEA	2.56	−144.5467	−0.8280	−22.53
PbSe–TGA	2.69	−238.4360	−0.8183	−22.27
PbSe–L-cys	2.71	−333.0133	−0.8071	−21.96
PbSe–MHA	2.55	−395.5201	−0.8035	−21.86
PbSe–TGC	2.69	−277.7001	−0.7976	−21.70
PbSe–MPA	2.57	−277.7024	−0.7903	−21.51

chemical methods demonstrate a good performance in the case of nanoparticles' properties modeling and also are accurate for various metal-containing species.[40–44] Theoretical calculations were performed using DFT simulations of model systems. To simplify the simulations, a single Pb atom was used with two capping molecules attached. Representative snapshots for TGA and MEA ligands interacted with Pb atom are shown in Fig. 5.

Pb–ligand complexes were calculated in order to predict the stability energies and to compare energies among various Pb–ligand systems. To characterize the investigated complexes the stability energy E_{ST} was calculated according to the following reaction,

$$M_{Pb^{2+}} + 2L \rightarrow ML_2 \quad (1)$$
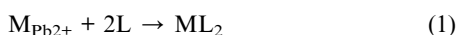
and then corresponding equation,

$$E_{ST} = E_{ML} - (E_M + E_L) \quad (2)$$

where E_{ML}, E_M and E_L denote the energies of the complex ML and its two components M and L. The components M and L are the metal of interest (Pb^{2+}) and a ligand, respectively. The ligands of interest were optimized for the conformation with minimum energy that is then used for the metal–ligand complex calculations. Geometry optimizations for ligands and Pb(II) salts were carried out without symmetry restrictions. The optimized structures of all the Pb(II) salts display a four-coordinate pseudo-trigonal bipyramidal bonding environment.

The calculated theoretical data (Table 5) reveal that MEA formed more stable complex with Pb^{2+} compared to other ligands. This complex is characterized by −22.53 eV stabilization energy that is in good agreement with experimental data (see Table 4) that were recorded as the daily stability of the QD solutions during the study (e.g., two months). The theoretical
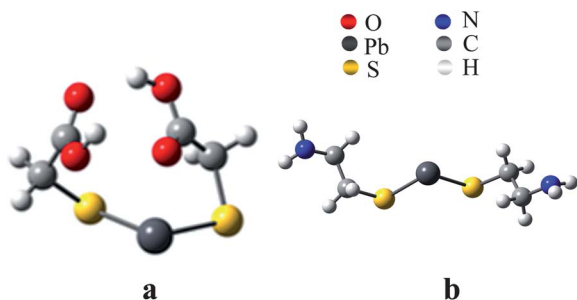
data for TGA-capped PbSe QDs (the second most stable) are also consistent with the experimental findings (see Tables 4 and 5). For the rest of the ligands, the order of experimental stabilities is not consistent with the theoretical values, which is attributed to indistinguishable differences among the daily stabilities of the QDs (e.g., stabilities varied only a day or two). However, the theoretical calculations support the experimental findings that the PbSe QDs capped with MPA, MHA, L-cys, and TGC are not as stable as those of MEA and TGA because of the instability of their Pb–thiolate complexes. The Pb–S bond lengths fall into the range of 2.55–2.71 Å.

3.5 Purification and re-dispersion of PbSe QDs

As mentioned earlier, PbSe QD solutions were purified to remove excess of the precursors with different solvents depending of thiol-ligand present on the nanocrystal surfaces. The results are shown in Table 6. Although DMSO is a non-toxic solvent, the reaction with PbSe QD solutions was exothermic increasing the temperature of the QD solutions up to 50 °C resulting in rapid precipitation. To avoid this effect, QD solutions were immersed in an ice bath to keep the temperature around 18–20 °C. For QDs capped with TGA and MPA (short chain ligands), DMSO ensured the effective precipitation of the QDs from solution to remove the unreacted components. However, when the carbon chain of the acid was increased to six, 2-propanol (1 : 0.5 ratio) was found to be the most suitable solvent for precipitation. In the case of L-cys- and MEA-capped QDs, the precipitation was carried out by mixing the QDs solution with acetone at 1 : 3 QD/acetone volume ratio. While MEA-capped QDs were successfully re-dispersed in water, those capped with L-cysteine could not, even in the presence of free ligand. The TGC-capped QDs could not be precipitated at room temperature since this ligand yielded highly water soluble QDs. In this case, the suspensions were forced to precipitate by heating in acetone, but the resulting residue could not be re-dispersed in water as occurred with L-cysteine. All QD solutions were purified a day after the preparation and immediately re-dispersed in water with an excess of the free ligands.

Fig. 6a–c show typical TEM images for TGA-capped PbSe QDs. Fig. 6a illustrates that unpurified bare QDs possess well-defined, uniform size distribution. Aggregation started in about 5 min after purification and re-dispersing the QDs in water at pH 7.8 (Fig. 6b). Within 30 min, QDs completely aggregated and fell out of the solution (Fig. 6c and d, right). This type of network formation (Fig. 6b and d) has been reported previously and used

Fig. 5 Optimized geometries of the (a) Pb–TGA complex and (b) Pb–MEA complex.

Table 6 Solvents and volume ratios used for purification of thiol-capped PbSe QDs

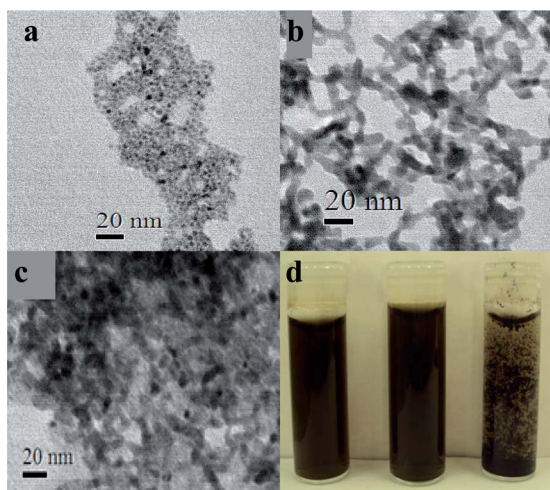| QD–Ligand	Solvent	QD : solvent ratio (v/v)
PbSe–MPA	DMSO	1 : 1
PbSe–MEA	Acetone	1 : 3
PbSe–TGA	DMSO	1 : 1
PbSe–MHA	2-Propanol	1 : 0.5
PbSe–L-cys	Acetone	1 : 3
PbSe–TGC	Acetone/heat	1 : 1

Fig. 6 TEM images for TGA-capped PbSe QDs. (a) Bare QDs, (b) purified and re-dispersed QDs in water—5 min later and (c) 45 min later; (d) photograph of purified PbSe QDs suspension in water. Left: bare QDs; middle: 5 min after re-dispersion; and right: 30 min after re-dispersion.

to obtain gels and aerogels from the thiol-capped QDs of CdTe.[46,47]

Similar experiments were conducted with MPA-capped PbSe QDs. It was found that the purified solutions were remarkably less stable (10–15 min) than TGA-capped QDs. To improve the colloidal stability in water, initially, the pH of the purified QDs suspension was increased to basic values, but the results were not successful since high pH only rendered the ligand more soluble. In the next stage, free ligand concentration in water was increased to improve the adsorption of the ligand on the QD surface and in due course the stability of the QDs. These experiments were performed with MPA, TGA and MEA-capped QDs that readily dispersed in water after purification. Table 7 shows the conditions used for re-dispersion and the stabilities for each ligand. It is clear that MEA-capped QDs were the most stable in solution. This result is also supported by the theoretical calculations (Table 5).

The results in Table 7 demonstrate that excess of free ligands are necessary in the solution to maintain ligand exchange on the QD surface. These results are also supported by those of Ji *et al.*[45] who indicated that the interaction of the ligands with CdSe nanocrystals was a desorption–adsorption process.[45] Although

Table 7 The extent of stability recorded for the purified PbSe QDs in the presence of excess of free ligands

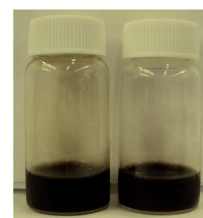|	Concentration of ligand/M	pH	Stability in the dark at 4 °C (day)
PbSe–MPA	0.01	7.3–7.5	9–12
	0.02	9.7–9.8	4
	0.04	7.1–7.5	1–2
PbSe–TGA	0.02	7.0–7.2	5
	0.02	8.0–8.2	2
	0.05	9.7–9.8	1
PbSe–MEA	0.02	7.35	45–47
	0.02	8.00	30
	0.02	9.82	13

Fig. 7 Picture of purified and concentrated MEA-capped PbSe QDs solution. Left: 800 ± 30 ppm and right: 1098 ± 26 ppm. Samples were re-dispersed in 0.05 M MEA solution at pH 7.0.

the presence of free ligands improved the stability of the PbSe QDs in solution, aggregation could not be completely avoided as they were highly susceptible to oxidation[9,39] resulting in the loss of Pb atoms and ligands from the QD surface.[36]

Attempts were also made to concentrate the MPA-, TGA-, and MEA-capped PbSe QD solutions after purification. To scale-up the concentration, bare QDs were precipitated and re-dispersed in a minimum volume of water (*ca.* 1 mL) with excess of free ligands. Fig. 7 shows the typical images from the purified concentrates of MEA-capped PbSe QDs that are stable for over two months.

4. Conclusion

In this study, synthesis of PbSe QDs was described in aqueous solution using thiol-containing ligands. The proposed method utilizes environmentally friendly precursors and solvents, and affords rapid synthesis at room temperature in a single step. The XRD patterns showed that all thiol-capped QDs possess a cubic rock salt structure regardless of the type of ligand. However, the experimental and theoretical results demonstrate that the stability of the PbSe QDs is dependent on multiple factors, such as the choice of ligand, pH, temperature and light exposure. A reasonable explanation for the observed colloidal instability is the growth of the nanocrystals, leading finally to the coagulation of massive particles and their aggregates. The stabilizers used (except of MEA and TGA) are not suitable to prevent this growth. The most stable QDs are produced by using MEA and TGA as they could inhibit this aggregation to some extent. The Pb–thiolate complexes of these ligands also exhibit the lowest stabilization energy among the other ligands used confirming that the stabilization energy of Pb–ligand complex plays an important role in determining the overall stability of the particular PbSe QDs. It is therefore concluded that more DFT calculations are necessary to find the optimal ligand and to expand the DFT calculations to the clusters of PbSe besides the single Pb atom–ligand model used in this study.

The synthesis presented here yields morphologically reproducible PbSe QDs. The presence of free ligands in the purified solutions of MEA- and TGA-capped PbSe QDs is critical to achieve prolonged stability. In addition, the method offers the ability to concentrate the QDs to desired levels easily. Surface modification or coating with inorganic and polymeric material is expected to provide added surface protection for improved stability. Studies are currently being conducted and the results will be addressed in a future publication.

Acknowledgements

References

1 C. B. Murray, S. Sun, W. Gaschler, H. Doyle, T. A. Betley and C. R. Kagan, *IBM J. Res. Dev.*, 2001, **45**, 47–56.

2 W. W. Yu, J. C. Falkner, B. S. Shih and V. L. Colvin, *Chem. Mater.*, 2004, **16**, 3318–3322.

3 I. C. Baek, S. I. Seok, N. C. Pramanik, S. Jana, M. A. Lim, B. Y. Ahn, C. J. Lee and Y. J. Jeong, *J. Colloid Interface Sci.*, 2007, **310**, 163–166.

4 H. Du, C. Chen, R. Krishnan, T. D. Krauss, J. M. Harbold, F. W. Wise, M. G. Thomas and J. Silcox, *Nano Lett.*, 2002, **2**, 1321–1324.

5 R. D. Schaller and V. I. Klimov, *Phys. Rev. Lett.*, 2004, **92**, 186601.

6 J. S. Steckel, S. Coe-Sullivan, V. Bulović and M. G. Bawendi, *Adv. Mater.*, 2003, **15**, 1862–1866.

7 G. Sarasqueta, K. R. Choudhury and F. So, *Chem. Mater.*, 2010, **22**, 3496–3501.

8 I. L. Medintz, H. T. Uyeda, E. R. Goldman and H. Mattoussi, *Nat. Mater.*, 2005, **4**, 435–446.

9 Q. Dai, Y. Zhang, Y. Wang, Y. Wang, B. Zou, W. W. Yu and M. Z. Hu, *J. Phys. Chem. C*, 2010, **114**, 16160–16167.

10 R. Kerner, O. Palchik and A. Gedanken, *Chem. Mater.*, 2001, **13**, 1413–1419.

11 F. S. Terra, G. M. Mahmoud, M. Nasr and M. M. E. Okr, *Surf. Interface Anal.*, 2010, **42**, 1239–1243.

12 J. Xu, J.-P. Ge and Y.-D. Li, *J. Phys. Chem. B*, 2006, **110**, 2497–2501.

13 S. Singh, K. Bozhilov, A. Mulchandani, N. Myung and W. Chen, *Chem. Commun.*, 2010, **46**, 1473–1475.

14 M. J. Mulvihill, S. E. Habas, I. Jen-La Plante, J. Wan and T. Mokari, *Chem. Mater.*, 2010, **22**, 5251–5257.

15 X. Gao, Y. Cui, R. M. Levenson, L. W. K. Chung and S. Nie, *Nat. Biotechnol.*, 2004, **22**, 969–976.

16 X. Zhou, Y. Kobayashi, V. Romanyuk, N. Ochuchi, M. Takeda, S. Tsunekawa and A. Kasuya, *Appl. Surf. Sci.*, 2005, **242**, 281–286.

17 S.-W. Kim, S. Kim, J. B. Tracy, A. Jasanoff and M. G. Bawendi, *J. Am. Chem. Soc.*, 2005, **127**, 4556–4557.

18 L. Etgar, E. Lifshitz and R. Tannenbaum, *J. Mater. Res.*, 2008, **23**, 899–903.

19 A. B. Fischer and Y. Skreb, *Arh. Hig. Rada Toksikol.*, 2001, **52**, 333–354.

20 N. Gaponik, D. V. Talapin, A. L. Rogach, K. Hoppe, E. V. Shevchenko, A. Kornowski, A. Eychmuller and H. Weller, *J. Phys. Chem. B*, 2002, **106**, 7177–7185.

21 Z. Arslan, M. Ates, W. McDuffy, M. S. Agachan, I. O. Farah, W. W. Yu and A. J. Bednar, *J. Hazard. Mater.*, 2011, **192**, 192–199.

22 M. J. Frisch, G. W. Trucks, H. B. Schlegel, G. E. Scuseria, M. A. Robb, J. R. Cheeseman, J. A. Montgomery, T. Vreven, K. N. Kudin, J. C. Burant, J. M. Millam, S. S. Iyengar, J. Tomasi, V. Barone, B. Mennucci, M. Cossi, G. Scalmani, N. Rega, G. A. Petersson, H. Nakatsuji, M. Hada, M. Ehara, K. Toyota, R. Fukuda, J. Hasegawa, M. Ishida, T. Nakajima, Y. Honda, O. Kitao, H. Nakai, M. Klene, X. Li, J. E. Knox, H. P. Hratchian, J. B. Cross, V. Bakken, C. Adamo, J. Jaramillo, R. Gomperts, R. E. Stratmann, O. Yazyev, A. J. Austin, R. Cammi, C. Pomelli, J. W. Ochterski, P. Y. Ayala, K. Morokuma, G. A. Voth, P. Salvador, J. J. Dannenberg, V. G. Zakrzewski, S. Dapprich, A. D. Daniels, M. C. Strain, O. Farkas, D. K. Malick, A. D. Rabuck, K. Raghavachari, J. B. Foresman, J. V. Ortiz, Q. Cui, A. G. Baboul, S. Clifford, J. Cioslowski, B. B. Stefanov, G. Liu, A. Liashenko, P. Piskorz, I. Komaromi, R. L. Martin, D. J. Fox, T. Keith, A. Laham, C. Y. Peng, A. Nanayakkara, M. Challacombe, P. M. W. Gill, B. Johnson, W. Chen, M. W. Wong, C. Gonzalez and J. A. Pople, *Revision C.02*, Gaussian, Inc., Wallingford, CT, 2004.

23 R. G. Parr and W. Wang, *Density Functional Theory of Atoms and Molecules*, Oxford University Press, New York, 1992.

24 Y. Zhao and D. G. Truhlar, *J. Chem. Phys.*, 2006, **124**, 224105.

25 C. Peng, P. Y. Ayala, H. B. Schlegel and M. J. Frisch, *J. Comput. Chem.*, 1996, **17**, 49–56.

26 M. S. Bakshi, P. Thakur, P. Khullar, G. Kaur and T. S. Banipal, *Cryst. Growth Des.*, 2010, **10**, 1813–1822.

27 I. Moreels, K. Lambert, D. De Muynck, F. Vanhaecke, D. Poelman, J. C. Martins, G. Allan and Z. Hens, *Chem. Mater.*, 2007, **19**, 6101–6106.

28 X. Wang, G. Xi, Y. Liu and Y. Qian, *Cryst. Growth Des.*, 2008, **8**, 1406–1411.

29 E. Smith and G. Dent, *Modern Raman Spectroscopy—A Practical Approach*, Wiley & Sons, Hoboken, NJ, 2005.

30 B. Schrader, *Infrared and Raman Spectroscopy, Methods and Applications*, VCH, Weinheim, 1995.

31 M. S. Abd El-sadek, J. Ram Kumar and S. Moorthy Babu, *Curr. Appl. Phys.*, 2010, **10**, 317–322.

32 S. W. Han, H. S. Han and K. Kim, *Vib. Spectrosc.*, 1999, **21**, 133–142.

33 C. Yufang, C. Zhang, H. Yejuan, L. Hailan, S. Pengtao, L. Chegbin, L. Shenglian and C. Qingyun, *Nanotechnology*, 2010, **21**, 125502.

34 J. K. Cooper, A. M. Franco, S. Gul, C. Corrado and J. Z. Zhang, *Langmuir*, 2011, **27**, 8486–8493.

35 Z. Peng, M. Liu, C. Yu, Z. Chai, H. Zhang and C. Wang, *Nanoscale*, 2010, **2**, 697–699.

36 I. Moreels, B. Fritzinger, J. C. Martins and Z. Hens, *J. Am. Chem. Soc.*, 2008, **130**, 15081–15086.

37 J. Aldana, Y. A. Wang and X. Peng, *J. Am. Chem. Soc.*, 2001, **123**, 8844–8850.

38 A. L. P. Cornacchio and N. D. Jones, *J. Mater. Chem.*, 2006, **16**, 1171–1177.

39 Q. Dai, Y. Wang, Y. Zhang, X. Li, R. Li, B. Zou, J. Seo, Y. Wang, M. Liu and W. W. Yu, *Langmuir*, 2009, **25**, 12320–12324.

40 T. Puzyn, B. Rasulev, A. Gajewicz, X. Hu, T. P. Dasari, A. Michalkova, H.-M. Hwang, A. Toropov, D. Leszczynska and J. Leszczynski, *Nat. Nanotechnol.*, 2011, **6**, 175–178.

41 D. Majumdar, S. Roszak and J. Leszczynski, *Chem. Phys. Lett.*, 2011, **501**, 308–314.

42 S. Schenk, P. Schwab, M. Dzierzawa and U. Eckern, *Phys. Rev. B: Condens. Matter*, 2011, **83**, 115128.

43 P. P. Favero, A. C. Ferraz. and R. Miotto, *Phys. Condens. Matter*, 2011, **23**, 045001.

44 B. Rasulev, D. Leszczynska and J. Leszczynski, Nanoparticles: Towards Predicting their Toxicity and Physico-Chemical Properties, in *Advanced Methods and Applications in Chemoinformatics: Research Progress and New Applications*, ed. E. A. Castro, A. K. Haghi, IGI Global, 2011, pp. 92–110.

45 X. Ji, D. Copenhaver, C. Sichmeller and X. Peng, *J. Am. Chem. Soc.*, 2008, **130**, 5726–5735.

46 N. Gaponik, A. Wolf, R. Marx, V. Lesnyak, K. Schilling and A. Eychmüller, *Adv. Mater.*, 2008, **20**, 4257–4262.

47 I. U. Arachchige and S. L. Brock, *J. Am. Chem. Soc.*, 2006, **128**, 7964–7971.